Ruthenium Trichloride Catalyst in Water Ru Colloids versus Ru Dimer Characterization Investigations

Anastasia Lebedeva, Brunno L Albuquerque, Josiel B Domingos, Jean-François Lamonier, Jean-Marc Giraudon, Pierre Lecante, Audrey Denicourt-Nowicki, Alain Roucoux

Ruthenium trichloride catalyst in water: Ru colloids *vs.* Ru dimer. Characterization investigations

Anastasia Lebedeva,[a] *Brunno L. Albuquerque,*[b, c] *Josiel B. Domingos,*[b] *Jean-François Lamonier,*[d] *Jean-Marc Giraudon,*[d] *Pierre Lecante,*[e] *Audrey Denicourt-Nowicki,*[a,*] *Alain Roucoux*[a,*]

[a] Univ Rennes, Ecole Nationale Supérieure de Chimie de Rennes, CNRS, ISCR-UMR 6226, F-35000 Rennes, France

[b.] LaCBio, Laboratory of Biomimetic Catalysis, Chemistry Department, Universidade Federal de Santa Catarina, Campus Trindade, 88040-900 Florianópolis, SC, Brazil

[c] LAMOCA, Laboratory of Molecular Catalysis, Chemistry Institute, Universidade Federal do Rio Grande do Sul, Campus do Vale, 91501-970 Porto Alegre, RS, Brazil

[d] Univ. Lille, CNRS, Centrale Lille, ENSCL, Univ. Artois, UMR 8181 - UCCS - Unité de Catalyse et Chimie du Solide, Lille, 59000, France

[e] Centre d'Elaboration des Matériaux et d'Etudes Structurales du CNRS, 9 Rue Marvig, BP 4347, 31055 Toulouse Cedex, France

Audrey.Denicourt@ensc-rennes.fr; Alain.Roucoux@ensc-rennes.fr

KEYWORDS. Ruthenium – Csp^3-H activation – Oxidation – Cycloalkanes – Water

ABSTRACT. An easy-to-prepare ruthenium catalyst obtained from ruthenium(III) trichloride in water demonstrates efficient performances in the oxidation of several cycloalkanes with high selectivity towards the ketone. In this work, several physico-chemical techniques were used to demonstrate the real nature of the ruthenium salt still unknown in water and to define the active species for this Csp^3-H bond functionalization. From Transmission Electron Microscopy analyses corroborated by SAXS analyses, spherical nanoobjects were observed with an average diameter of 1.75 nm, thus being in favor of the formation of reduced species. However, further investigations, based on X-ray scattering and absorption analyses, showed no evidence of the presence of a metallic Ru-Ru bond, proof of zerovalent nanoparticles, but the existence of Ru-O and Ru-Cl bonds, and thus the formation of a water-soluble complex. The EXAFS (extended X-ray absorption fine structure) spectra revealed the presence of an oxygen-bridged diruthenium complex $[Ru(OH)_xCl_{3-x}]_2(\mu\text{-}O)$ with a high oxidation state in agreement with catalytic results. This study constitutes a significant advance to determine the true nature of the $RuCl_3 \cdot 3H_2O$ salt in water and proves once again the invasive nature of the electron beam in microscopy experiments, routinely used in nanochemistry.

INTRODUCTION

The activation and the functionalization of the kinetically inert Csp^3-H bonds constitute one of the main challenges of synthetic chemistry.[1-3] In that field, the selective and controlled oxidation of relatively cheap hydrocarbons constitutes a relevant value-creating synthetic methodology, to produce pertinent oxyfunctionalized feedstocks for various industrial branches, ranging from polymer synthesis to pharmaceutical chemistry.[4-5] One of the obvious and large-scaled industrial application remains the liquid-phase oxidation

of cyclohexane into cyclohexanone and cyclohexanol (KA oil),[6-7] key intermediates for the production of nylon-6 and nylon-6,6.[8] This process, catalyzed by soluble cobalt salts acting as homogeneous species, is generally performed under drastic temperature and pressure conditions (413-433K, 1-2MPa), owing to the high energy required to cleave the Csp^3-H bond.[9] Furthermore, cyclohexane oxidation presents very low yields (< 5-10%) to limit the overoxidation products and high waste production.[10]

Despite recent advances in this field,[11] the development of more efficient and eco-responsible catalytic methodologies[3] for the oxidation of cycloalkanes remains of interest in regards to the great demand for the oxyfunctionalized raw materials. Over the various metals, ruthenium remains a pertinent candidate, being an oxophilic metal,[12-13] and thus suitable for oxidation reactions,[14-15] and presents a cheaper cost than other noble metals with quite stable prices over time.

Very recently, our team has used ruthenium (III) trichloride hydrate in neat water, as an original and relevant catalyst for the oxidation of various cycloalkanes in pure biphasic (water/substrate) conditions.[16] High conversions and nearly complete selectivities toward the corresponding ketones were obtained. However, the reaction requires quite long reaction times (9h), within fractional additions of oxidant in six times. In the present paper, easier and practical reaction conditions have been developed and evaluated on the oxidation of various cyclic alkanes. Moreover, the previous promising results led our group to ask the following question: What are the real characteristics of these ruthenium species? Could we define the structure of this catalyst? To answer these questions and to better understand the nature of the ruthenium active species, we carried out some essential spectroscopic and microscopic techniques, including X-ray absorption and diffusion

(scattering) analyses. In the present paper, the results of all these investigations are discussed and contributed to solve the problem of the true nature of the ruthenium species provided in water for this Csp^3-H functionalization reaction.

EXPERIMENTAL SECTION

Materials. Ruthenium (III) trichloride hydrate, $RuCl_3.3H_2O$, was provided by STREM Chemicals or Sigma-Aldrich. All cyclic alkanes and the aqueous *tert*-butylhydroperoxide solution (Luperox TBH70X, 70% wt. in H_2O) were purchased from Sigma-Aldrich, Acros Organics or TCI Chemicals. Water was distilled twice before use.

Synthesis of the colloidal ruthenium suspension. The $RuCl_3.3H_2O$ (0.2 mmol) salt was dissolved in 10 mL of ultra-pure water, resulting in a homogeneous solution with a concentration of 0.02 mol L^{-1}. The obtained strongly acidic colloidal solution (pH = 1.5-1.6) was stirred overnight and could then be directly used for oxidation reactions.

Catalytic experiments. The oxidation of various cycloalkanes was performed at room temperature in the presence of the ruthenium colloidal suspension. In a typical reaction, a 100 mL round bottom flask was charged with 3 mL of ultra-pure water, 2.23 mmol (1 eq.) of substrate and 892 µL (0.0178 mmol, 0.008 eq.) of the ruthenium colloidal suspension. The flask was closed and the reaction medium was stirred for 5 minutes in order to homogenize the solution. Then the aqueous solution of *tert*-butylhydroperoxide (1 + 2 x 0.5 eq.) was added using a syringe every hour under stirring. The adequate amount was withdrawn with a syringe and added in one time, *via* the septum. At the end of the reaction, the reaction products were extracted with diethyl ether (2 x 3 mL). Then, 1.5 mL of the obtained organic solution was charged in the GC vial. The conversion and the selectivity were determined using chlorobenzene

as internal standard, using TRACE GC ULTRA apparatus with a FID detector equipped with a Thermo Fisher HP5-MS capillary column (30 m, 0.25 i.d., 0.5 f.t.). The injector and detector temperatures were set at 250°C. Products identification was performed by comparison of their retention times with commercial products.

DLS analysis. The hydrodynamic size of nanoparticle aggregates was directly measured in water solution by a dynamic light scattering (DLS) technique using a DelsaNano C (Beckman counter).

TEM experiments. Transmission electron microscopy (TEM) images were recorded with a JEOL TEM 100CXII electron microscope operated at an acceleration voltage of 100 kV. The samples were prepared by the addition of a drop of the stabilized colloid in water on a copper grid coated with a porous carbon film. The size distributions were determined for around 200 particles, through a manual analysis of enlarged micrographs with ImageJ software using Microsoft Excel to generate histograms of the statistical distribution and a mean diameter. High resolution TEM analysis was recorded by a JEOL JEM 2010 UHR electron microscope with lanthanum hexaboride source (LaB_6).

XPS analysis. X-ray photoelectron spectroscopy measurements were acquired with VG ESCALAB 220XL spectrometer at room temperature using Al-Kα radiation (1486.6 eV) as the excitation X-ray source and calibrated by setting the C 1s peak to 285.0 eV. During the experiment, the pressure in the analysis chamber was maintained at 10^{-7} Pa. The data processing was performed using the CasaXPS software. The solid sample for the analysis was prepared by lyophilization of the initial catalyst solution by means of CryoNext freeze-dryer. The lyophilization consists of the sublimation of frozen water in vacuum overnight. Then, the sample prepared as a pellet was fixed to the sample holder by means of

double-sided adhesive tape. The decomposition of Ru $3d_{5/2}$ and Ru $3d_{3/2}$ core levels was performed considering the following methodology : an applied Shirley background and an asymmetric line shape in the form of a tail-dampened Lorentzian asymmetric line shape given represented in LF (α,β,w,m) form, where α and β define the spread of the tail on either side of the Lorentzian component, m the width of the Gaussian used to convolute the Lorentzian curve and w the tail-dampening parameter. The Casa XPS fitting parameters were LF(0.9, 1.2, 25,280) and LF(0.9, 1.2, 25, 280) for the simulation of the Ru $3d_{5/2}$ and Ru $3d_{3/2}$ core levels, respectively.

SAXS experiments were performed on the SAXS1 beamline of the Brazilian Synchrotron Light Laboratory (LNLS – Campinas, SP, Brazil). The solutions were loaded into a temperature-controlled vacuum flow-through cell composed of two mica windows separated by 1 mm, normal to the beam. The collimated beam (k = 1.55 Å) crossed the sample through an evacuated flight tube and was scattered to a Pilatus 300 K 2D detector (Dectris) and a 2D CCDmarCCD 165 detector, respectively. The incident beam was detected at 500 mm distance on the SAXS1 beamline, (silver behenate was used for sample-to-detector distance calibration), to achieve the scattering vector range q (from 0.1 to 5 nm^{-1}).

The ***in situ*** **XAS analyses** were performed on the XDS Beamline at the Brazilian Synchrotron Light Source (LNLS) in Campinas. The spectra were acquired at room temperature in transmission mode with three ionization chambers using a Si (311) double-crystal monochromator and a toroidal focusing mirror. A standard Ru foil (metallic Ru) was used to perform energy calibration in all scans. Four to six spectra were collected to improve the signal-to-noise ratio. Each spectrum was acquired in a range of 21.940−22.950 keV with 2-6 s/point. The data have been processed using the IFEFFIT

and Demeter packages (Athena and Artemis). The data were calibrated using Ru foil as reference. The Ruthenium K-edge was chosen at 22.117 keV and the data acquired in transmission mode using a custom designed Teflon sample holder sealed on both sides with Kapton tape.

Wide Angle X-ray Scattering (WAXS) measurements were performed at CEMES Toulouse, on the lyophilized sample. Measurements of the X-ray intensity scattered by the samples irradiated with graphite monochromatized molybdenum KR (0.071069 nm) radiation were performed using a dedicated two-axis diffractometer. Time for data collection was typically 20 h for a set of 457 measurements collected at room temperature in the range $0° < \theta < 65°$. Data were reduced in order to extract the structure-related component of WAXS, the so-called reduced intensity function, normalized to a number of atoms corresponding to the size of the particles, and Fourier transformed allowing for radial distribution function (RDF) analysis.

RESULTS AND DISCUSSION

Catalytic oxidation of cycloalkanes. The catalytic performances of the ruthenium catalyst were evaluated in the oxidation of various cyclic alkanes possessing 5 to 12 carbons at room temperature, using practical and industrially suitable reaction conditions (shorter reaction times and three-time oxidant additions). The reaction was performed in the presence of *tert*-butylhydroperoxide as a safer and eco-responsible oxidant[17] and in water as a suitable industrial green solvent.[18] The catalytic results in terms of activity and selectivity, determined by Gas Chromatography analyses, using these novel parameters are gathered in Table 1.

Table 1. Catalytic performances of the ruthenium catalyst in the cycloalkane oxidation reaction in neat water[a]

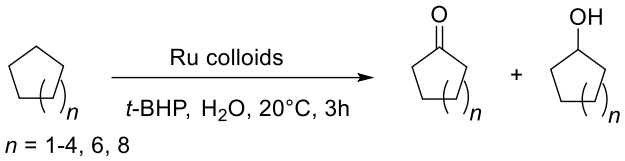

Entry	Cycloalkane	Conversion (%) [b]	Selectivity (%) [b]	Conditions
Reference[c]	Cyclohexane	97	90	Previous work[16]
1	Cyclopentane	46	89	This work
2	Cyclohexane	53	90	This work
3	Cycloheptane	61	100	This work
4	Cyclooctane	41	98	This work
5	Cyclodecane	26	96	This work
6	Cyclododecane[c]	29	90	This work

[a] Reaction conditions: Cycloalkane (2.23 mmol, 1 eq.), *t*-BHP (1 + 2 x 0.5 eq.), Substrate/Metal = 125, 3 mL H_2O, 20°C, 1 h per *t*-BHP addition, total reaction time = 3h. [b] Determined by GC analysis using chlorobenzene as internal standard. [c] 2 mL of ethyl acetate as co-solvent. [c] Reaction conditions: Cyclohexane (2.23 mmol, 1 eq.), *t*-BHP (6 x 0.5 eq.), Substrate/Metal = 125, 3 mL H_2O, 20°C, 1.5 h per *t*-BHP addition, total reaction time = 9h.

First, whatever the size of the substrate is, high selectivity towards the corresponding ketone ranging from 90 to 100% was achieved, with negligible or no formation of the respective alcohol. However, the conversion is dependent on the size of the ring, reaching an optimum of 60% in 3h for cycloheptane (Entry 3). For cyclopentane, a 45% conversion was obtained in 3 h, affording cyclopentanone, well-known as a key intermediate for the production of Jasmone. The conversion decreases with the increase in

the size of the cycle from C7 to C10, as already reported in the literature with some catalysts.[19-20] This difference in reactivity could be explained by a significant decrease in the solubility of the cycloalkane within water (from 156 mg L^{-1} for C5 to 0.33 mg L^{-1} for C10),[21] and also by a more difficult abstraction of the cycloalkane hydrogen in the first step of the reaction mechanism. In the case of the lipophilic cyclododecane, ethyl acetate was used as a co-solvent for the oxidation reaction, leading to the formation of cyclododecanone with a 23% conversion in 3 h. Undoubtedly, the aqueous solution of ruthenium trichloride proved to be a pertinent catalyst for the selective oxidation of cycloalkanes in neat water, under mild reaction conditions, compared to recently described catalysts.[19-20] Comparing with previous works (Table 1, reference), these novel conditions afforded promising conversions (53% in 3h *vs*. 97% in 9h), with a comparable selectivity in ketone (90%). Thus, higher conversions could be achieved in the presence of this ruthenium catalyst through the modulation of various reaction parameters (amount of oxidant and reaction time), as already reported by the authors.[16] In the absence of chemical reducing agent, which should provide zerovalent species, the real nature of the active species was investigated, using various characterization techniques.

Transmission electron microscopic (TEM) studies. The microscopy (TEM) investigations were carried out to determine the morphology and the size of the active species before catalytic oxidation tests. Well-dispersed spherical metallic particles, with an average diameter of 1.75 ± 0.25 nm, were observed. The distribution histogram (Fig. 1) revealed that 90% of the particles possess a small size between 1.5 and 2 nm.

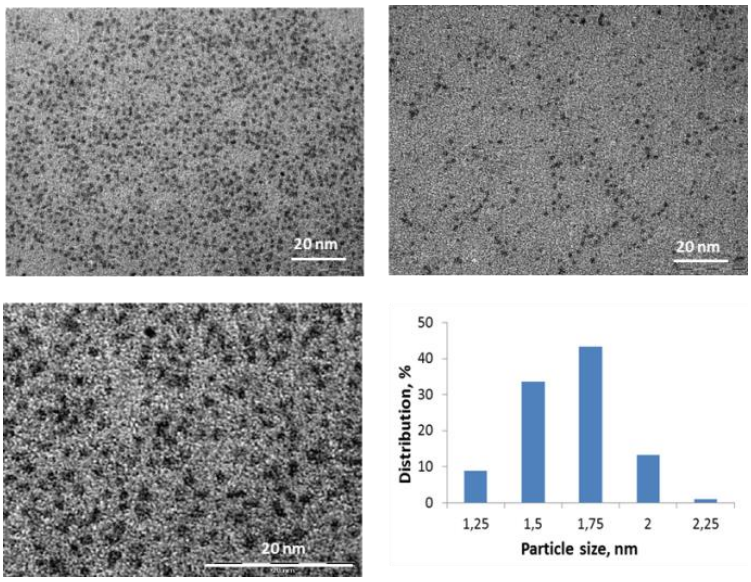

Figure 1. TEM images (Scale bar = 20 nm) and size distribution of Ru colloids before catalytic oxidation applications

The as prepared ruthenium colloids were also identified by high resolution transmission electron microscopy (HR-TEM) experiments to better understand the sample atomic structure (Fig. 2). The HR-TEM micrographs showed the presence of relatively well-organized crystalline objects with interplanar distances of 0.234, 0.214 and 0.206 nm corresponding to the (100), (002) and (101) planes lattice of ruthenium (0) (ICDD-JCPDS n° 06-0663). These observations are in agreement with the results obtained in the literature for zerovalent ruthenium nanoparticles synthesized by chemical reduction of $RuCl_3$ with sodium borohydride.[22-23] All these microscopic results, in terms of morphologies and sizes of the particles, are similar to the ones reported in our previous works,[16] thus showing the good reproducibility of the methodology for the nanoparticles preparation.

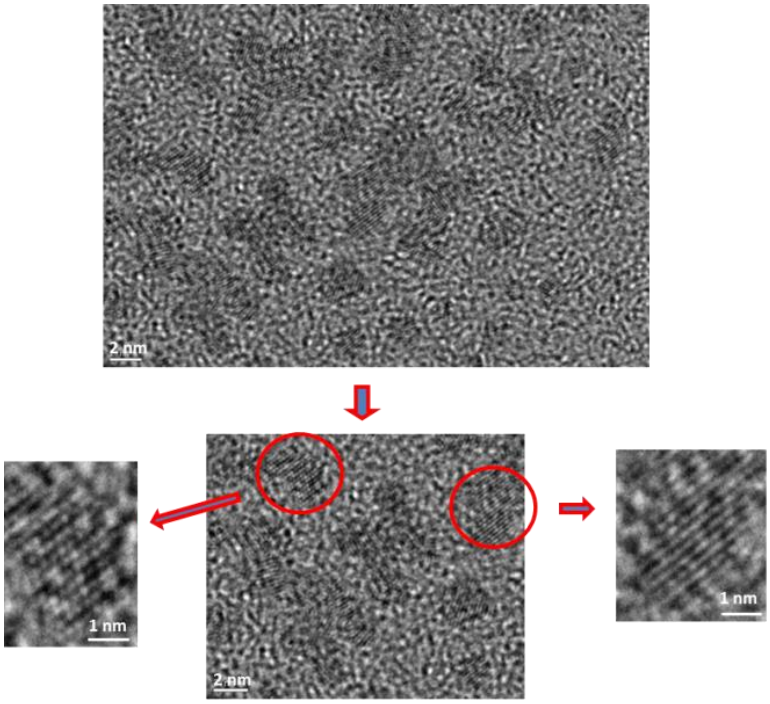

Figure 2. High resolution transmission electron micrographs of ruthenium colloids (Scale bar =2 nm)

Small angle X-ray scattering (SAXS). Additionally, the ruthenium colloids were also analyzed by Synchrotron based Small Angle X-ray Scattering (SAXS) analysis (Fig. 3). The data were fitted with the "sphere" model, accounting the particle morphology, as well as the "Beaucage Power Law" model, which includes the scattering from agglomerates, as recently described by Cardoso *et al.*[24] From the log-normal size distribution (Fig. 3b), the average diameter of the particles is centered on 0.96 nm with a dispersion (σ) of 0.357, which is in good agreement with TEM measurements.

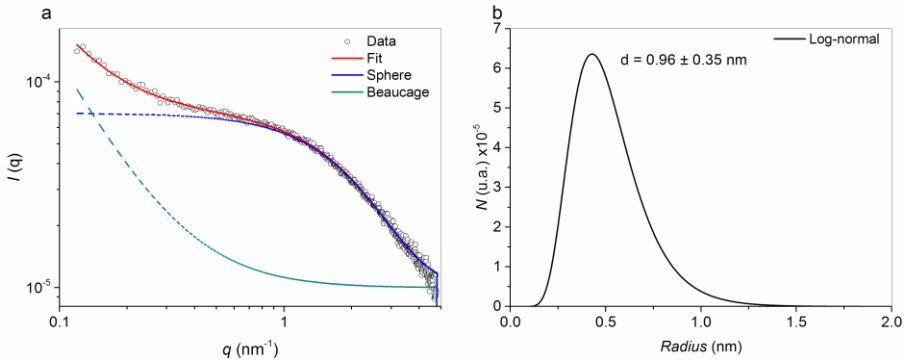

Figure 3. a) SAXS spectrum of ruthenium colloids and b) Size distribution obtained by "Sphere" modelling of SAXS fitting.

Based on this first set of experiments such as Transmission Electron microscopy and, SAXS analysis, we could presume the formation of reduced metal particles obtained by ligands displacement and reductive elimination, and stabilized in water by chloride ions (subshell), themselves surrounded by hydronium ions H_3O^+ (outer shell) in the strong acidic media. This proposed electronical double-layer around the catalyst core was also confirmed by dynamic light scattering (DLS) analyses, which gives a hydrodynamic diameter of 5 nm, higher than the one obtained by TEM analyses. This size difference could probably be attributed to the presence of the ionic environment around the metal particle. However, additional characterization techniques (XPS, XAS, WAXS) were carried out for a better understanding of the catalytic system through the determination of the metal species nature.

X-Ray photoelectron spectroscopic (XPS) analysis. The surface composition of the catalyst was determined by X-ray photoelectron spectroscopy. The survey spectrum of ruthenium colloids is presented on Fig. 4a and various peaks for Ru 3d, Ru 3p, Cl 2p, O 1s and C 1s (reference) are observed at binding energies values of 280-284 eV, 460-480 eV, 198 eV, 530 eV and 285 eV, respectively. Concerning the ruthenium species, the Ru 3d region was first investigated in order to determine the ruthenium oxidation state, as generally performed in the publications.[25] As shown in Fig. 4b, the Ru 3d core level clearly shows two apparent maxima located at 282.3 and 286.5 eV. Even if these components overlap with those of the C1s core level precluding easy identification of Ru species, the binding energy (BE) value of Ru $3d_{5/2}$ fits well with the value of 282.4 eV reported by D.J. Morgan,[25] considering an average value of $RuCl_3$ and $Ru(OH)_3$, as well as the Ru $3d_{3/2}$ component positioned at a distance of + 4.17 eV. Moreover, no contribution of a peak located at 279.9eV attributed to Ru(0) was observed (Fig. 4b). Furthermore, the absence of a shoulder in the low BE range precludes the presence of RuO_2 as the BE of Ru $3d_{5/2}$ is expected to be shifted towards a lower value to that of $RuCl_3/Ru(OH)_3$, namely at 280.7 eV. To conclude, the envelope based on Ru 3d + C 1s contribution is believed to be composed only of a Ru(III) component. Finally, the XPS Ru 3p core-level was studied. Fig. 4c shows the well-resolved doublet ($3p_{5/2}$ and $3p_{3/2}$ at 463.9 and 486 eV, respectively) leading to an energy separation of 22.1. According to the literature,[25] as well as the atomic ratio of the OH^- contribution to that of Cl^- (O1s OH)/(Cl 2p) = 9.32/9.17 close to one, these binding energies values can be attributed to the presence of Ru^{3+} species as ruthenium trichloride salt $RuCl_3$ and/or ruthenium hydroxide $Ru(OH)_3$. The Cl 2p signal (Fig. 4d) consists of two components, namely Cl $2p_{3/2}$ and $2p_{1/2}$, located at 198.4 and 200 eV, with an energy separation of 1.6 eV. These values are in agreement with mineral chlorine. Besides, The O 1s envelope, exhibited in Fig. 4e, can be

decomposed into two peaks. The first one located at 533.3 eV corresponds to H_2O adsorbed on the surface, while the second one at 531.7 eV is assigned to OH^- ions in interaction with Ru^{3+}. Based on these different results and the existence of chloro species under equilibrium in solution,[26] a $Ru(OH)_xCl_{(3-x)}$ structure may be postulated. This assumption is supported by the value of the experimental (Cl 2p + O 1s (OH))/(Ru 3d) atomic ratio of 3.8 close to the expected one of 3.0.

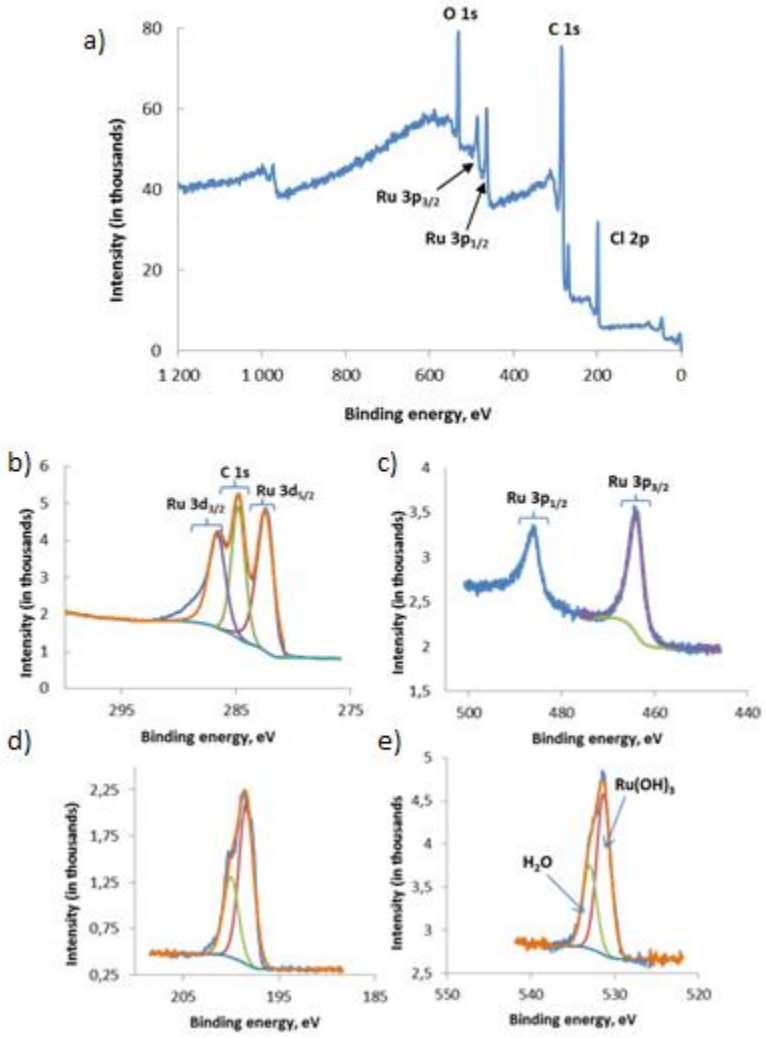

Figure 4. X-ray photoelectron spectroscopic (XPS) analysis of ruthenium colloids a) Survey XPS spectrum b) Ru 3d, c) Ru 3p, d) Cl 2p and e) O 1s regions

To resume, XPS information are in favor of the presence of a high-valent ruthenium complex with a $Ru(OH)_xCl_{(3-x)}$ type-structure in the colloidal solution ($RuCl_3 \cdot 3H_2O$ in water), instead of zerovalent particles as supposed from our previous investigations based on analyses usually used in the nanocatalysis field such as transmission microscopy experiments (TEM, TEM-HR).

X-ray absorption spectroscopy (XAS). Ruthenium K-edge XAS analysis were performed in transmission mode on the colloidal ruthenium solution and compared to surfactant-stabilized ruthenium zerovalent nanoparticles (Ru@HEA16Cl), prepared by chemical reduction of the metal precursor ($RuCl_3 \cdot 3H_2O$), in the presence of sodium borohydride ($NaBH_4$) as chemical reductant and *N*,*N*-dimethyl-*N*-cetyl-*N*-(2-hydroxyethyl)ammonium chloride (HEA16Cl surfactant) as protective agent.[27] A ruthenium metal foil (Ru foil) was also used as reference for zerovalent Ru species, along with the $RuCl_3 \cdot 3H_2O$ salt.

XANES experiments. Firstly, the XANES (X-ray absorption near edge structure) spectrum of the ruthenium colloidal solution was recorded in the range of energies from 22100 eV to 22150 eV and compared to those of commercial $RuCl_3 \cdot 3H_2O$ salt, Ru@HEA16Cl, and Ru foil used as reference materials (Fig. 5).

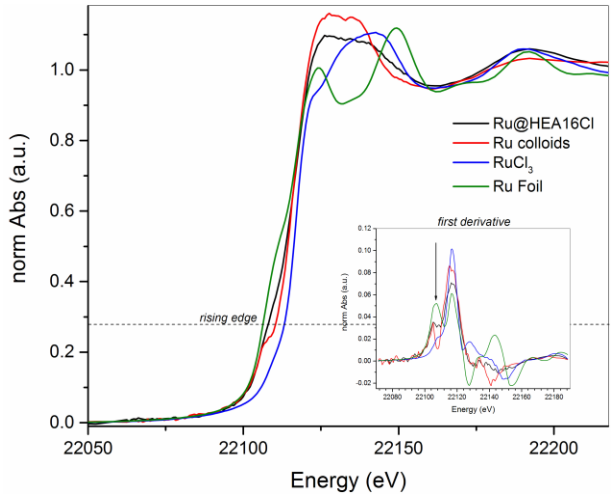

Figure 5. Normalized XANES spectra for the Ru K-edge of the ruthenium colloidal solution (red) compared with commercial salt (blue), Ru@HEA16Cl nanoparticles (black) and metallic ruthenium foil (green). Inset, the first derivative of the XANES data highlighting the rising edge feature in our samples

Based on fingerprinting of the Ru samples, it is possible to check that $RuCl_3$ is consumed during its solubilisation in water to afford ruthenium colloids as an evidence of the hydrolysis of the starting metal salt. Studies on the formation of Ru nanoparticles in aqueous media by Pantani,[28] Troitskii *et al.*[29] as well as Kahn,[26, 30] showed that polymerized forms of $[RuCl(H_2O)_5]^{2+}$ can be formed in solution among other species present in the equilibria. Since the XANES is sensitive to the local coordination and the chemical environment, our conclusion is that some of the chlorine on the $RuCl_3$ structure are replaced by oxygen atoms, either OH^- or H_2O, according to XPS data. Moreover, a rising-edge shift could be detected for the samples showed in Fig. 5, in the case of ruthenium colloids, thus indicating a higher oxidation state of the metal species in this sample compared to the Ru foil or to the Ru@HEA16Cl nanospecies.[31] The position was determined by the first derivative of the XANES spectra, Fig 5. inset. The rising edge

shifts using Ru foil as standard was 1.3 eV for Ru@HEA16Cl, 3.3 eV for Ru colloids and 6 eV for $RuCl_3$. The reduced ruthenium nanoparticles, Ru@HEA16Cl, showed a shift close to the ruthenium foil, which indicates a partial surface passivation of ruthenium nanoparticles. In fact, a Ru-O contribution can be observed due to a sample preparation at air. Finally, the shift is similar for commercial $RuCl_3$, and we could presume that the oxidation state of the ruthenium in the colloidal solution is 3+. The XANES spectrum for the colloids shows some similar features to those obtained by Ohta et *al.*[32-33] and was attributed to RuO_h complex structure. A shoulder is also visible on the Ru colloids sample in the rising edge (pre-edge) of the spectrum. According to literature, this phenomenon is associated with the quadrupole transition of electrons from 1s level to the higher 3d level and may be presented due to the coordination chemistry of the ruthenium.[34]

EXAFS experiments. The ruthenium foil was fitted using a single shell approach with a fixed coordination number of 12,[35-36] to obtain the value of the standard amplitude, which was 0.73 and used for the fitting of the samples. The fitting range for *k* and R was respectively 3 to 12.63 **Å**$^{-2}$ and 1.75 to 3 **Å**. The Debye-Waller factor and the bond length agree with the crystal standard (ICSD 54236, obtained by X-Ray Diffraction) and are shown in Table 2. The $RuCl_3$ was also fitted and its parameters are summarized in Table 2 using X-Ray diffraction standard (ICSD 22091). From the comparison between the FT EXAFS spectra for the ruthenium samples and the $RuCl_3$ (Fig. 6 a,b), the amplitude in the Ru-Cl peak is lower in the ruthenium colloids, characterizing a less amount of Cl atoms coordinated to the Ru, as determined by the EXAFS fit in Table 2. In the case of the Ru@HEA16Cl, the absence of the Ru-Cl contribution is evident.

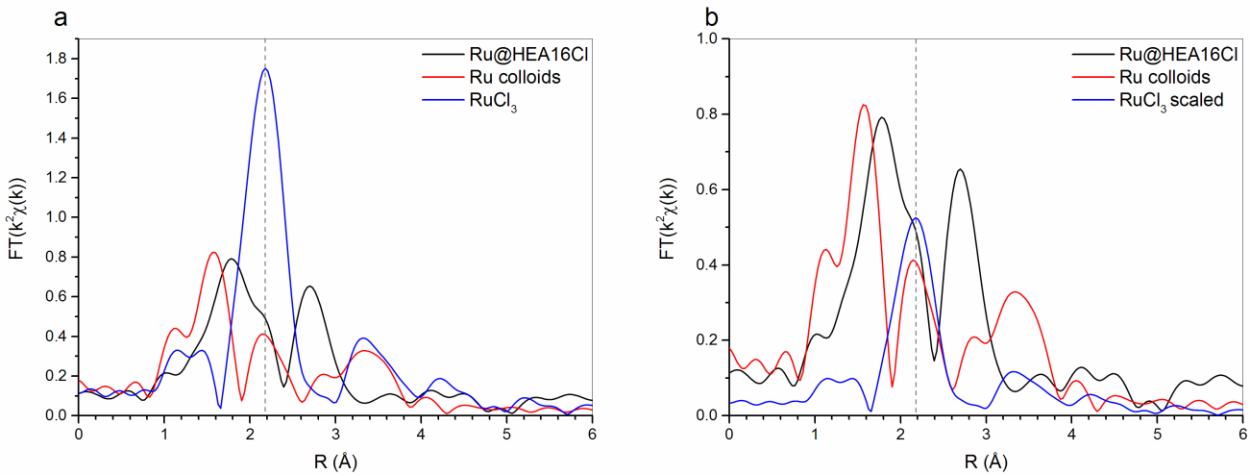

Figure 6. For EXAFS experiments, the Ru colloids and Ru@HEA16Cl samples were acquired in solution form and the $RuCl_3$ as a powder a) Phase-corrected Fourier-transformed k^2-weighted EXAFS spectra of the Ru samples and b) Scaled-down $RuCl_3$ data in the sake of comparison.

Table 2. EXAFS parameters obtained after fitting of Ru colloids and Ru@HEA16Cl.

Parameters	Samples			
	Ru foil	$RuCl_3$	Ru colloids	Ru@HEA16Cl
N_{Ru-O}	-	-	3.1(1)	4.5(2)
R_{Ru-O} (Å)	-	-	1.824(1)	1.782(2)
σ^2_{Ru-O} (Å^2)	-	-	0.0030(2)	0.0084(8)
N_{Ru-Cl}	-	3*	1.72(2)	-
R_{Ru-Cl} (Å)	-	2.312(2)	2.363(3)	-
σ^2_{Ru-Cl} (Å^2)	-	0.002(1)	0.0070(6)	-
N_{Ru-O2}	-	-	1.39(9)	-
R_{Ru-O2} (Å)	-	-	3.396(1)	-
σ^2_{Ru-O2} (Å^2)	-	-	0.0016(2)	-
N_{Ru-Ru}	12*	-	-	4.2(3)
R_{Ru-Ru} (Å)	2.641(1)	-	-	2.667(2)
σ^2_{Ru-Ru} (Å^2)	0.0031(1)	-	-	0.0088(6)

*Fixed values[24].

The EXAFS spectrum of the ruthenium colloid sample obtained in transmission mode was fitted and is consisted with an octahedral dimeric structure, as seen in XANES, with an oxygen atom in a bridge form and three other oxygen atoms from hydroxy groups according to XPS investigations. The data were fitted in *k* range from 2.8 to 11 Å^{-2} and in R range from 0.75 to 3.8 Å (Fig. 7a and b), respectively. Even though the signal is noisy in high k ranges, probably due to the aqueous nature of the sample, the data fitted well with R-factor of 0.016 and χ_ν^2 of 40.25.

The Ru-Cl bond in the colloidal form showed a small expansion in comparison with the $RuCl_3$ sample (0.05 Å), probably due to the difference in the coordination structure (2.312 *vs.* 2.363 Å respectively). The bond length of the bridging oxygen (3.648 Å for Ru-O-Ru) is consistent with a value of 3.724 Å observed in the 2,2'-bipyridine (bpy) ruthenium aqua-complex $[(bpy)_2(H_2O)Ru(\mu\text{-}O)Ru(H_2O)(bpy)_2]^{4+}$.[32,37] The different chemical environment might be responsible for the slight bond shortening and a difference was also observed for the Ru-Cl bond length.

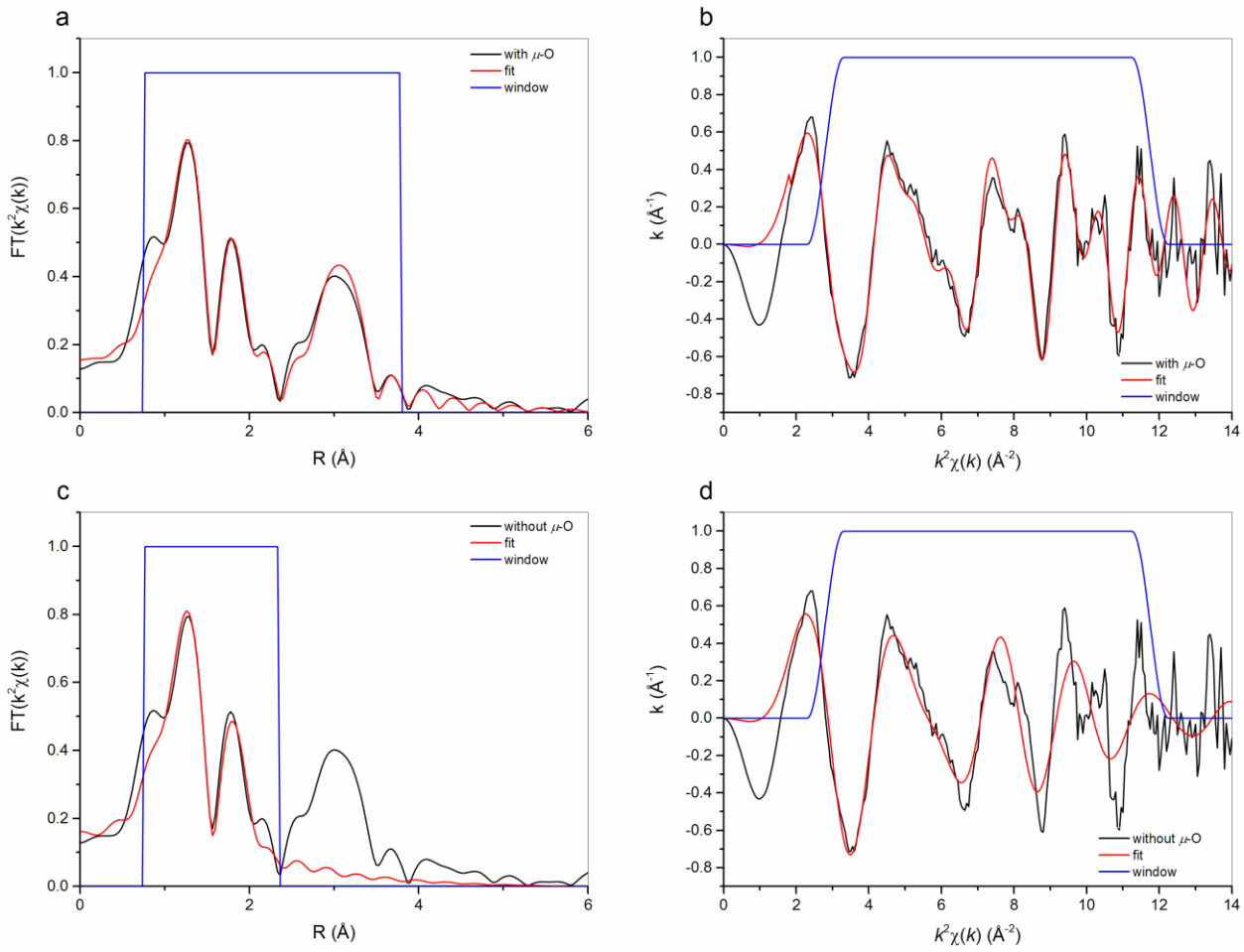

Figure 7. Fourier-transformed k^2-weighted EXAFS spectra and k^2-weighted EXAFS spectra and respective fits for (a,b) ruthenium colloids and (c,d) ruthenium colloids without the μ-O bridge.

The average coordination number gave an insight about the composition of the compound. From the basic stoichiometry resulted from the EXAFS fitting, and considering a dimeric octahedral structure as pointed out in the XANES fingerprinting, the diruthenium complex $[Ru(OH)_3Cl_2]_2(\mu\text{-}O)$ (Fig. 8) could be proposed as a starting precursor of high valent ruthenium species according to the literature,[31-32] which are catalytically active towards Csp^3-H bond oxidation.[19] A different approach to the data fitting was performed discarding the presence of a μ-O bridge, (Figure 7 c,d) which resulted in a poorer quality of the fit. The R-factor increased to 0.021 and the χ_v^2 increased to 76.36. The graph in Fig. 7d shows the fitting discarding the μ-O bridge misses the data points in $k > 4$ Å^{-2}.

Many studies have been reported to clarify oxidation mechanisms involving ruthenium-oxo species.[38] In the case of the oxidation of hydrocarbons by *t*-BHP, many investigations prove that the oxidation is not due to *tert*-butoxyl (*t*BuO$^{\cdot}$) and *tert*-butylperoxyl (*t*BuOO$^{\cdot}$) radicals but to high-valent oxo-species derived from low valent ruthenium species as Ru-OO*t*Bu followed by the cleavage of the O-O bond by protonolysis.[38] As reported by Thummel *et al*.,[39] these high valence species (Ru^{IV} or Ru^{V}) in acid media are often postulated as intermediate catalysts in water oxidation for concomitant O=O formation. In fact, $Ru^{V}ORu^{V}$ has been identified as a key step in solution.[40-41] This way could explain the pivotal role of O_2 discussed in the previous proposed radical mechanism, which is based on 1) the formation of cyclohexylperoxy intermediate from cyclohexyl radicals and molecular oxygen, and 2) the decomposition of cyclohexylhydroperoxide in the corresponding ketone as supported by the recent literature.[42-44] Moreover, the observed high selectivity towards ketones (Table 1) could be also associated to oxo ruthenium species, which have already been reported in alcohol oxidation.[45] Finally, starting

from ruthenium materials, single site ruthenium catalysts[46-47] could also be proposed even if, in our case, no proof could consolidate this hypothesis.

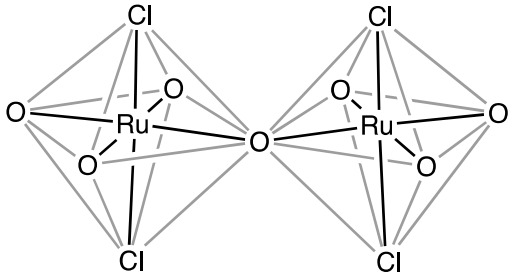

Figure 8. Proposed structure for the high-valent oxygen-bridged diruthenium complex based on the hydrolysis of $RuCl_3 \cdot 3H_2O$. Hydrogens were omitted for clarity.

For the sake of comparison, the Ru@HEA16Cl was fitted in *k* range from 3 to 11.7 $Å^{-2}$ and in R range from 1.22 to 2.82 Å (Figure 9a,b, respectively). The statistical parameters of this fit are in good agreement with the model, with a R-factor of 0.015 and χ_v^2 of 23.03. Ruthenium is a high oxophilic metal and strong reducing agents such as $NaBH_4$ are required for its reduction even if passivation, providing an oxidized shell, could not be excluded in water. From the average coordination number, we can conclude that ruthenium nanoparticles are formed with a core-shell structure, with a metallic core and oxidized domains. From EXAFS studies, we can distinguish the different nature of ruthenium species. In reductive conditions, ruthenium nanoparticles were obtained and characterized by the presence of the Ru-Ru metal bond in contrast to the formation of an oxygen-bridged ruthenium complex for the colloidal solution easily obtained by dissolving $RuCl_3 \cdot 3H_2O$ in water.

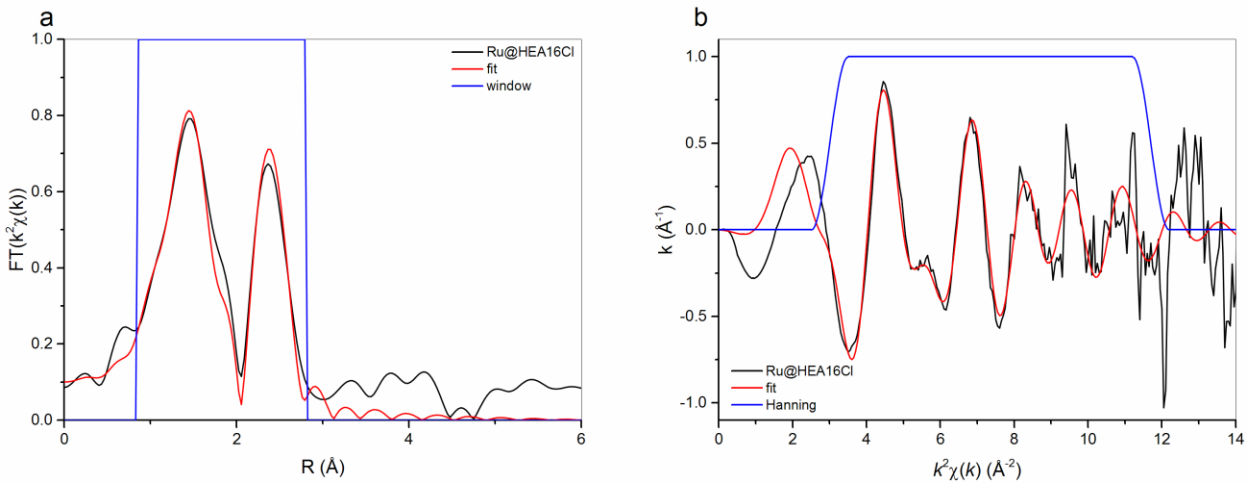

Figure 9. a) Fourier-transformed k^2-weighted EXAFS spectra and b) k^2-weighted EXAFS spectra and respective fits for Ru@HEA16Cl.

Wide angle X-ray scattering (WAXS). To support these results, wide-angle X-ray scattering (WAXS) analyses were conducted on both samples, the colloidal suspension obtained by solubilization of $RuCl_3$ in water and the chemically reduced and surfactant-stabilized ruthenium nanoparticles (Ru@HEA16Cl). This technique, widely reported in the literature for NPs of noble metals,[48-49] allows obtaining information on the distribution of metal-metal distances within a homogeneous assembly. Indeed, a well-defined radial distribution function (RDF) corroborates the presence of well-crystallized nanoparticles. The comparison with the theoretical data obtained by modeling helps in determining the crystalline structure of the particles (position and intensity of the peaks are compared), as well as the coherent length (longest metal-metal distance). The RDF of both samples (ruthenium colloids and Ru@HEA16Cl) were compared to the reference one of the Ru nanoparticles (Fig. 10). The WAXS analyzes of the lyophilized ruthenium colloids did not show the compact hexagonal structure (hcp) of metallic ruthenium species and the presence of the distance of the Ru-Ru bond of 0.267 nm.[50] Moreover, these

ruthenium-based species are not highly crystalline and have a rather amorphous structure. Finally, a Ru-O bond (d = 0.195 nm) could be detected,[51] as well as a Ru-Cl bond (d = 0.230 nm). In contrast, drastic changes were observed for the Ru@HEA16Cl sample, even if analysis is complicated due to strong contributions. However, considering the short distances related to the bonding of Ru, any Ru-Cl contribution can now be excluded. Moreover, the 0.26-0.30 nm range, where the Ru-Ru metallic bonding distance is expected, is now consistent with such metallic bonding. The RDF in this range is however broader than in purely metallic particles and the shorter distance consistent with Ru-O can still be observed. All these elements point to a composite system including small metallic cores and oxidized domains, in agreement with EXAFS.

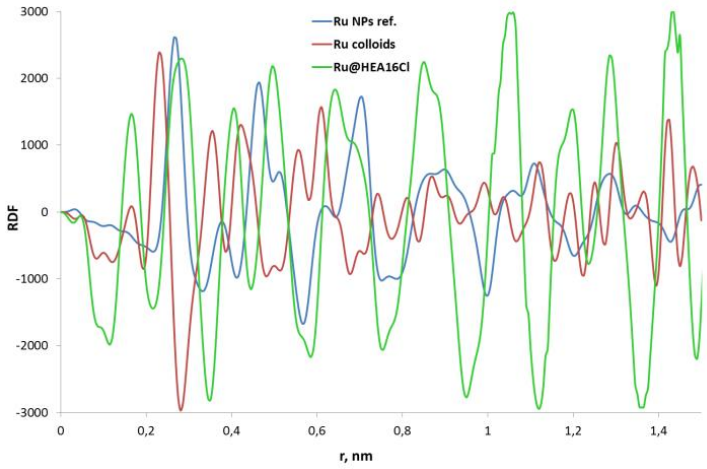

Figure 10. Radial distribution function obtained from WAXS analyzes: ruthenium colloids (red), Ru@HEA16Cl (green) and ruthenium nanoparticles as reference (blue)

CONCLUSION

A ruthenium colloidal solution, easily prepared by dissolution of $RuCl_3.3H_2O$ metal precursor in water, proved to be active and selective for the oxidation of various cycloalkanes, in the presence of *tert*-butylhydroperoxide in water. Based on the preliminary investigations carried out by means of high resolution transmission electron microscopy, the formation of reduced metallic nanospecies of Ru with an average size of 1.75 nm was initially proposed. However, further studies, based on X-ray scattering and absorption analyses (XPS, EXAFS, XANES, WAXS), revealed the presence in aqueous solution of a Ru-O-Ru bridge and a dimeric octahedral structure of $[Ru(OH)_3Cl_2]_2(\mu\text{-}O)$ with a high oxidation state based on Ru-O and Ru-Cl bonds which is well-known to provide in acidic water solution high-valent Ru═O species in which the Ru-O bonds have a double-bond character. Thus, the formation of reduced nanoparticles as suggested by HR-TEM analyses could be attributed to the electron beam emitted during the analysis. Synchrotron X-Rays can also be a source for the formation of spherical nano-objects in liquid phase due to the high incident energy of the photons of about 8 keV (SAXS1-LNLS). This phenomenon, already reported in the literature,[52-54] allows us to show again the limit of microscopy experiments and SAXS in the nanocatalysis field.

Synchrotron X-Rays can also be a source for the formation of spherical nano-objects in liquid phase due to the high incident energy of the photons of about 8 keV (SAXS1-LNLS). This phenomena, already reported in the literature,[52-55] allows us to show again the limit of microscopy experiments and SAXS in the nanocatalysis field.

Finally, commercial ruthenium chloride in water provides various complexes in equilibrium and has been the subject of numerous statements since more than 40 years. Due to the complexity of identified species, these catalytic and spectroscopic investigations constitute new advances in the understanding of the molecular structure of the ruthenium species present in aqueous media and reveals new opportunities for the catalytic Csp^3-H functionalization of hydrocarbons.

AUTHOR INFORMATION

Corresponding Authors

E-mail: Audrey.Denicourt@ensc-rennes.fr

E-mail: Alain.Roucoux@ensc-rennes.fr

ORCID

Audrey Denicourt-Nowicki: 0000-0003-2992-8403

Alain Roucoux : 0000-0002-3283-8241

Jean-François Lamonier : 0000-0002-6420-1296

Jean-Marc Giraudon : 0000-0002-9535-6629

Pierre Lecante : 0000-0001-6337-6855

Brunno Lange Albuquerque: 0000-0002-8188-5837

Author Contributions

The manuscript was written through contributions of all authors. All authors have given approval to the final version of the manuscript. ‡These authors contributed equally. (match statement to author names with a symbol)

Funding Sources

The authors declare no competing financial interest Notes

ACKNOWLEDGMENT

The authors thank Patricia Beaunier from Sorbonne Université for performing TEM analyses and Simon Pardis for XPS analysis (UMR 8181– Unité de Catalyse et Chimie du Solide), and MSER for financial support of PhD thesis of A. Lebedeva. The authors are also grateful to the Brazilian Synchrotron Light Laboratory (LNLS), under proposals SAXS1-19004 and XDS- 20160243, for the beam time usage.

SYNOPSIS

Ruthenium(III) trichloride in water proved to be a relevant and efficient catalyst for the oxidation of several cycloalkanes with high selectivity towards the corresponding ketone. Various physico-chemical investigations allow to determine a dimeric structure of $[Ru(OH)_3Cl_2]_2(\mu\text{-}O)$ as catalytic precursor of high-valent active species in agreement with the Csp^3-H bond functionalization of hydrocarbons.

GRAPHICAL ABSTRACT

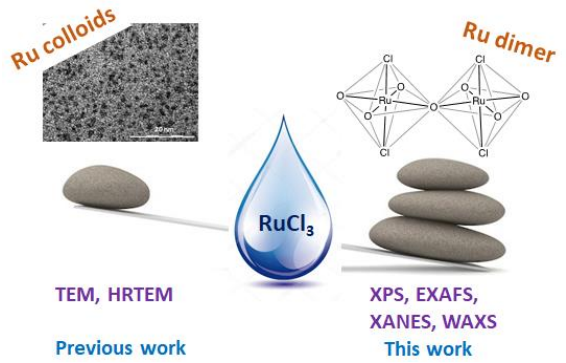

REFERENCES

1. Shteinman, A. A., Activation and selective oxy-functionalization of alkanes with metal complexes: Shilov reaction and some new aspects. *J. Mol. Catal. A* **2017,** *426*, 305-315.
2. Shilov, A. E.; Shul'pin, G. B., Activation of C−H Bonds by Metal Complexes. *Chem. Rev.* **1997,** *97* (8), 2879-2932.
3. Xie, J.; Zhu, C., *Sustainable C(sp3)-H Bond Functionalization*. Springer Berlin Heidelberg: 2016.
4. Roduner, E.; Kaim, W.; Sarkar, B.; Urlacher, V. B.; Pleiss, J.; Gläser, R.; Einicke, W.-D.; Sprenger, G. A.; Beifuß, U.; Klemm, E.; Liebner, C.; Hieronymus, H.; Hsu, S.-F.; Plietker, B.; Laschat, S., Selective Catalytic Oxidation of C-H Bonds with Molecular Oxygen. *ChemCatChem* **2013,** *5* (1), 82-112.
5. Caron, S.; Dugger, R. W.; Ruggeri, S. G.; Ragan, J. A.; Ripin, D. H. B., Large-Scale Oxidations in the Pharmaceutical Industry. *Chem. Rev.* **2006,** *106*, 2943-2989.
6. Suresh, A. K.; Sharma, M. M.; Sridhar, T., *Ind. Engin. Chem. Res.* **2000,** *39*, 3958-3997.
7. Cyclohexanol and Cyclohexanone. In *Ullmann's Encyclopedia of Industrial Chemistry*, Musser, M. T., Ed. Wiley-VCH: Weinheim, 2000.
8. Schuchardt, U.; Calvarlho, W. A.; Spinace, E. V., Why is Interesting to Study Cyclohexane Oxidation? *Synlett* **1993,** *10*, 713-718.
9. Sheldon, R. A.; Kochi, J. K., In *Advances in Catalysis*, Eley, H. P. D. D.; Paul, B. W., Eds. Academic Press: 1976; Vol. 25, pp 272-413.
10. Sheldon, R. A.; Kochi, J. K., *Metal-Catalyzed Oxidations of Organic Compounds*. Academic press: New York.
11. Crabtree, R. H., Introduction to Selective Functionalization of C−H Bonds. *Chem. Rev.* **2010,** *110* (2), 575-575.
12. Tan, Q.; Wang, G.; Long, A.; Dinse, A.; Buda, C.; Shabaker, J.; Resasco, D. E., Mechanistic analysis of the role of metal oxophilicity in the hydrodeoxygenation of anisole. *J. Catal.* **2017,** *347*, 102-115.

13. Tyrlik, S. K.; Kurzak, K.; Randzio, S. L., Reactions of commercial ruthenium chlorides with O-donor ligands. Reactions with water: u.v.-vis. investigation of soluble products; analysis, thermogravimetry and an i.r. study of precipitated solids. *Transition Met. Chem.* **1995,** *20* (4), 330-337.
14. Nunes, G. S.; Alexiou, A. D. P.; Toma, H. E., Catalytic oxidation of hydrocarbons by trinuclear μ-oxo-bridged ruthenium-acetate clusters: Radical versus non-radical mechanisms. *J. Catal.* **2008,** *260* (1), 188-192.
15. Luo, X.; Wang, Z.; Chen, L.; Wang, X.; Wu, B., Facile Synthesis, Characterization and Catalytic Activity of Ruthenium-Containing Mesoporous Molecular Sieves. *Catal. Lett.* **2009,** *132* (3), 450.
16. Denicourt-Nowicki, A.; Lebedeva, A.; Bellini, C.; Roucoux, A., Highly Selective Cycloalkane Oxidation in Water with Ruthenium Nanoparticles. *ChemCatChem* **2016,** *8* (2), 357-362.
17. Corma, A.; Iborra, S.; Velty, A., Chemical Routes for the Transformation of Biomass into Chemicals. *Chem. Rev.* **2007,** *107* (6), 2411-2502.
18. Prat, D.; Wells, A.; Hayler, J.; Sneddon, H.; McElroy, C. R.; Abou-Shehada, S.; Dunn, P. J., CHEM21 selection guide of classical- and less classical-solvents. *Green Chem.* **2016,** *18*, 288-296
19. Acharyya, S. S.; Ghosh, S.; Adak, S.; Tripathi, D.; Bal, R., Fabrication of CuCr2O4 spinel nanoparticles: A potential catalyst for the selective oxidation of cycloalkanes via activation of Csp3–H bond. *Catal. Commun.* **2015,** *59*, 145-150.
20. Pillai, U. R.; Sahle-Demessie, E., Vanadium phosphorus oxide as an efficient catalyst for hydrocarbon oxidations using hydrogen peroxide. *New J. Chem.* **2003,** *27* (3), 525-528.
21. Yalkowsky, S. H.; He, Y.; Jain, P., *Handbook of Aqueous Solubility Data*. CRC Press: Boca Raton, 2010.
22. Anantharaj, S.; Jayachandran, M.; Kundu, S., Unprotected and interconnected Ru0 nano-chain networks: advantages of unprotected surfaces in catalysis and electrocatalysis. *Chem. Sci.* **2016,** *7* (5), 3188-3205.
23. Li, Y.; Huang, Y., Low-temperature, seed-mediated synthesis of monodispersed hyperbranched PtRu nanoparticles and their electrocatalytic activity in methanol oxidation. *J. Mater. Chem.* **2012,** *22* (25), 12461-12464.
24. de Oliveira, J. F. A.; Cardoso, M. B., Partial Aggregation of Silver Nanoparticles Induced by Capping and Reducing Agents Competition. *Langmuir* **2014,** *30* (17), 4879-4886.
25. Morgan, D. J., Resolving ruthenium: XPS studies of common ruthenium materials. *Surf. Interface Anal.* **2015,** *47* (11), 1072-1079.
26. Taqui Khan, M. M.; Ramachandraiah, G.; Rao, A. P., Ruthenium(III) chloride in aqueous solution: electrochemical and spectral studies. *Inorg. Chem.* **1986,** *25* (5), 665-670.
27. Nowicki, A.; Le Boulaire, V.; Roucoux, A., Nanoheterogeneous Catalytic Hydrogenation of Arenes: Evaluation of the Surfactant-Stabilized Aqueous Ruthenium(0) Colloidal Suspension. *Adv. Synth. & Catal.* **2007,** *349* (14-15), 2326-2330.
28. Pantani, F., The behaviour of ruthenium trichloride in aqueous solutions. *J. Less Common Met.* **1962,** *4* (2), 116-123.
29. Troitskii, S. Y.; Fedotov, M. A.; Kochubei, D. I.; Novgorodov, B. N.; Chuvilin, A. L.; Likholobov, V. A., Investigation of the formation process of nanosized particles of Ru(III). *J. Struct. Chem.* **2007,** *48* (1), 144-149.

30. Khan, M. M. T.; Ramachandraiah, G.; Shukla, R. S., Ruthenium(III) chloride in aqueous solution: kinetics of the aquation and anation reactions of the chloro complexes. *Inorg. Chem.* **1988,** *27* (19), 3274-3278.
31. Ishizuka, T.; Kotani, H.; Kojima, T., Characteristics and reactivity of ruthenium–oxo complexes. *Dalton Trans.* **2016,** *45* (42), 16727-16750.
32. Okamoto, K.; Miyawaki, J.; Nagai, K.; Matsumura, D.; Nojima, A.; Yokoyama, T.; Kondoh, H.; Ohta, T., Structural Study on Highly Oxidized States of a Water Oxidation Complex [RuIII(bpy)2(H2O)]2(μ-O)4+ by Ruthenium K-Edge X-ray Absorption Fine Structure Spectroscopy. *Inorg. Chem.* **2003,** *42* (26), 8682-8689.
33. Okamoto, K.; Takahashi, T.; Kohdate, K.; Kondoh, H.; Yokoyama, T.; Ohta, T., Characterization of the ruthenium–dinitrogen tetraamine complexes by XAFS spectroscopy. *J. Synchrotron Radiat.* **2001,** *8* (2), 689-691.
34. Getty, K.; Delgado-Jaime, M. U.; Kennepohl, P., Assignment of pre-edge features in the Ru K-edge X-ray absorption spectra of organometallic ruthenium complexes. *Inorg. Chim. Acta* **2008,** *361* (4), 1059-1065.
35. Frenkel, A., Solving the 3D structure of metal nanoparticles. In *Zeitschrift für Kristallographie - Crystalline Materials*, 2007; Vol. 222, p 605.
36. N. S. Marinkovic; K. Sasaki; Adtic, R. R., *Zastita Materijala* **2016,** *57*, 101-109.
37. Jurss, J. W.; Concepcion, J. J.; Butler, J. M.; Omberg, K. M.; Baraldo, L. M.; Thompson, D. G.; Lebeau, E. L.; Hornstein, B.; Schoonover, J. R.; Jude, H.; Thompson, J. D.; Dattelbaum, D. M.; Rocha, R. C.; Templeton, J. L.; Meyer, T. J., Electronic Structure of the Water Oxidation Catalyst cis,cis-[(bpy)2(H2O)RuIIIORuIII(OH2)(bpy)2]4+, The Blue Dimer. *Inorg. Chem.* **2012,** *51* (3), 1345-1358.
38. Murahashi, S.-I.; Zhang, D., Ruthenium catalyzed biomimetic oxidation in organic synthesis inspired by cytochrome P-450. *Chem. Soc. Rev.* **2008,** *37* (8), 1490-1501.
39. Tong, L.; Thummel, R. P., Mononuclear ruthenium polypyridine complexes that catalyze water oxidation. *Chem. Sci.* **2016,** *7* (11), 6591-6603.
40. Hurst, J. K., Water oxidation catalyzed by dimeric μ-oxo bridged ruthenium diimine complexes. *Coord. Chem. Rev.* **2005,** *249* (3), 313-328.
41. Binstead, R. A.; Chronister, C. W.; Ni, J.; Hartshorn, C. M.; Meyer, T. J., Mechanism of Water Oxidation by the μ-Oxo Dimer [(bpy)2(H2O)RuIIIORuIII(OH2)(bpy)2]4+. *J. Am. Chem. Soc.* **2000,** *122* (35), 8464-8473.
42. Hermans, I.; Nguyen, T. L.; Jacobs, P. A.; Peeters, J., Autoxidation of Cyclohexane: Conventional Views Challenged by Theory and Experiment. *ChemPhysChem* **2005,** *6* (4), 637-645.
43. Hermans, I.; Jacobs, P. A.; Peeters, J., Understanding the autoxidation of hydrocarbons at the molecular level and consequences for catalysis. *J. Mol. Catal. A* **2006,** *251* (1), 221-228.
44. Hermans, I.; Jacobs, P. A.; Peeters, J., To the Core of Autocatalysis in Cyclohexane Autoxidation. *Chem. Eur. J.* **2006,** *12* (16), 4229-4240.
45. Roecker, L.; Meyer, T. J., Hydride transfer in the oxidation of alcohols by [(bpy)2(py)Ru(Q)]2+. A kH/kD kinetic isotope effect of 50. *J. Am. Chem. Soc.* **1987,** *109* (3), 746-754.
46. Concepcion, J. J.; Jurss, J. W.; Norris, M. R.; Chen, Z.; Templeton, J. L.; Meyer, T. J., Catalytic Water Oxidation by Single-Site Ruthenium Catalysts. *Inorg. Chem.* **2010,** *49* (4), 1277-1279.

47. Zong, R.; Thummel, R. P., A New Family of Ru Complexes for Water Oxidation. *J. Am. Chem. Soc.* **2005,** *127* (37), 12802-12803.
48. Ortiz, N.; Hammons, J. A.; Cheong, S.; Skrabalak, S. E., Monitoring Ligand-Mediated Growth and Aggregation of Metal Nanoparticles and Nanodendrites by In Situ Synchrotron Scattering Techniques. *ChemNanoMat* **2015,** *1* (2), 109-114.
49. Martínez-Prieto, L. M.; Rakers, L.; López-Vinasco, A. M.; Cano, I.; Coppel, Y.; Philippot, K.; Glorius, F.; Chaudret, B.; van Leeuwen, P. W. N. M., Soluble Platinum Nanoparticles Ligated by Long-Chain N-Heterocyclic Carbenes as Catalysts. *Chem. Eur. J.* **2017,** *23* (52), 12779-12786.
50. Tristany M.; Chaudret B.; Dieudonné P.; Guari Y.; Lecante P.; Matsura V.; Moreno-Mañas M.; Philippot K.; Pleixats, R., Synthesis of Ruthenium Nanoparticles Stabilized by Heavily Fluorinated Compounds. *Adv. Funct. Mater.* **2006,** *16* (15), 2008-2015.
51. Martinez-Prieto, L. M.; Ferry, A.; Rakers, L.; Richter, C.; Lecante, P.; Philippot, K.; Chaudret, B.; Glorius, F., Long-chain NHC-stabilized RuNPs as versatile catalysts for one-pot oxidation/hydrogenation reactions. *Chem. Commun.* **2016,** *52* (26), 4768-4771.
52. Wahl, R.; Mertig, M.; Raff, J.; Selenska-Pobell, S.; Pompe, W., Electron-Beam Induced Formation of Highly Ordered Palladium and Platinum Nanoparticle Arrays on the S Layer of Bacillus sphaericusNCTC 9602. *Adv. Mater.* **2001,** *13* (10), 736-740.
53. Dang, Z.; Shamsi, J.; Palazon, F.; Imran, M.; Akkerman, Q. A.; Park, S.; Bertoni, G.; Prato, M.; Brescia, R.; Manna, L., In Situ Transmission Electron Microscopy Study of Electron Beam-Induced Transformations in Colloidal Cesium Lead Halide Perovskite Nanocrystals. *ACS Nano* **2017,** *11* (2), 2124-2132.
54. Ohkubo, Y.; Kageyama, S.; Seino, S.; Nakagawa, T.; Kugai, J.; Ueno, K.; Yamamoto, T. A., Mass production of highly loaded and highly dispersed PtRu/C catalysts for methanol oxidation using an electron-beam irradiation reduction method. *J. Exp. Nanosci.* **2016,** *11* (2), 123-137.
55. Plech, A.; Kotaidis, V.; Siems, A.; Sztucki, M., Kinetics of the X-ray induced gold nanoparticle synthesis. *Phys. Chem. Chem. Phys.* **2008,** *10* (26), 3888-3894.